Smart Structures and Systems, *Vol. 31*, *No. 1* (*2023*) *69-78*
https://doi.org/10.12989/sss.2023.31.1.069

A novel smart criterion of grey-prediction control for practical applications

Z.Y. Chen [1], Ruei-yuan Wang[*1], Yahui Meng[**1] and Timothy Chen[***2]

[1] *School of Science*, *Guangdong University of Petrochemical Technology*, *Maoming 525000*, *Guangdong*, *China*
[2] *California Institute of Technology*, *Pasadena*, *CA 91125*, *USA*

(*Received March 27*, *2022*, *Revised August 7*, *2022*, *Accepted September 2*, *2022*)

Abstract. The purpose of this paper is to develop a scalable grey predictive controller with unavoidable random delays. Grey prediction is proposed to solve problems caused by incorrect parameter selection and to eliminate the effects of dynamic coupling between degrees of freedom (DOFs) in nonlinear systems. To address the stability problem, this study develops an improved gray-predictive adaptive fuzzy controller, which can not only solve the implementation problem by determining the stability of the system, but also apply the Linear Matrix Inequality (LMI) law to calculate Fuzzy change parameters. Fuzzy logic controllers manipulate robotic systems to improve their control performance. The stability is proved using Lyapunov stability theorem. In this article, the authors compare different controllers and the proposed predictive controller can significantly reduce the vibration of offshore platforms while keeping the required control force within an ideal small range. This paper presents a robust fuzzy control design that uses a model-based approach to overcome the effects of modeling errors. To guarantee the asymptotic stability of large nonlinear systems with multiple lags, the stability criterion is derived from the direct Lyapunov method. Based on this criterion and a distributed control system, a set of model-based fuzzy controllers is synthesized to stabilize large-scale nonlinear systems with multiple delays.

Keywords: grey predictive robotic system; ocean platform; time delays and fuzzy controller

1. Introduction

Offshore platforms are typical offshore technical structures for oil and gas drilling. External pressure due to harsh environments such as waves, wind, ice, and earthquakes is unavoidable (Wang *et al*. 2013, Hasan *et al*. 2010). Operating on offshore platforms can cause vibration and affect the health of the structure. Passive (Zhang *et al*. 2022a, b), semi-active (Li *et al*. 2002, Zhang *et al*. 2020) and active strategies (Zhang *et al*. 2020) were studied and applied to the management of offshore structures (Zhang *et al*. 2017). Among them, active control has attracted much attention due to its high efficiency. A number of active controls have been proposed for offshore platforms protected with active mass damping devices (AMD), including sample data controls (Sakthivel *et al*. 2014), management expectations and feedback (Ma *et al*. 2009), $H\infty$ control (Xiao *et al*. 2022, Xu *et al*. 2022, 2023, Chen 2014a), H2 control (Lu *et al*. 2022), the slider (Zhang *et al*. 2014) *et al*. In the first case, the external load and delay (Lu *et al*. 2022, Chen *et al*. 2022) is an important factor to consider.

Today, the above theories and other good methods are widely used in engineering technology (Cheng *et al*. 2022, Fu *et al*. 2022, Gu *et al*. 2022, Han *et al*. 2022a, b, 2023, Li *et al*. 2021, Li and Geng 2023, Lu *et al*. 2022, Ma and Xu 2023, Sun *et al*. 2021, Zhao *et al*. 2022). However, these methods, especially control technology have been used to control systems with known mathematical models through simulation. Furthermore, the designs of these methods are mainly focused on the control of single-input single-output (SISO) systems. When these methods are applied to the operation of practical nonlinear systems (Cheng *et al*. 2022) is a multiple-input multiple-output (MIMO) system, which cannot effectively improve its control performance due to the inability to eliminate the dynamic coupling effect between the degrees of freedom in the system. Therefore, these methods need to be modified to achieve reasonable control performance for controlling robotic systems in practical applications. On the other hand, advanced control often requires large control gains and is prone to fluctuations. Therefore, many researchers have focused their research on the benefits of combining advanced design and model-free fuzzy logic control (FLC) in practical nonlinear systems. The challenge of determining appropriate membership functions and obfuscation rules remains a major problem for researchers. To eliminate this problem, Procyk and Mamdani (1979) figured out constructing fuzzy rules to manipulate a class of nonlinear servo systems. However, there is no guarantee that the rules are unclear. To address this problem, Chang (2010) proposed his self-organizing adaptive fuzzy controller for three- and two-DOF rehabilitation robots. Therefore, there is no guarantee that fuzzy rules are appropriate.

*Corresponding author, Dr.,
E-mail: rueiyuan@gmail.com
**Co-corresponding author, Mr.,
E-mail: mengyahui@gdupt.edu.cn
***Co-corresponding author, Mr.,
E-mail: t13929751005@gmail.com

ISSN: 1738-1584 (Print), 1738-1991 (Online)

In general, better control performance can be achieved for complex MIMO robotic systems by using two parameters instead of one as the FLC input variable. Therefore, this study includes the strengths and grey prediction algorithms of the above-mentioned drivers (Peng and Dong 2011, Shen *et al*. 2019) Development of Improved Advanced and Adaptive Fuzzy Predictive Controllers for Robotic Systems.

Many of today's technological problems arise from highly complex, high-dimensional, and stochastic technological, social, and environmental processes. The field of networked systems (also known as large systems) is very broad, encompassing both the basic theory of modeling, optimization, and control, as well as some specific aspects and applications. Especially the marine platform system not only includes various time control conditions, but also has a high degree of freedom of the system. As offshore oil rigs are located offshore and far from the mainland, the working conditions of offshore oil rigs are very difficult. In recent years, remote monitoring, network communication and distributed computing in marine engineering have attracted more and more attention. Therefore, the proposed controller outperforms the peer-to-peer architecture in controlling sea-level vibration. Over the years, several studies have focused on connected vibration control of offshore platforms. Considering the loop delay in the vibration control of the offshore platform network, a variable interval delay controller, a reliable fault-tolerant controller and a predictive controller are developed. However, these items do not include packaging loss or debris. Using marine equipment in harsh marine environments, network communications can be worse than on land, so occasional delays, packet loss, and interference become more severe and should be carefully considered. At the same time, given the application limitations of marine technology, offshore platform vibration control must be physically feasible and cost-effective. In this paper, we propose a grid vibration control model for offshore platforms that suffers from delays, mass disturbances, and discontinuities in the sensor-controller and controller-actuator channels. In this model, two buffers are designed to sort incoming packets and generate the packet with the oldest generation time. Based on the proposed model, we design an optimal predictive compensation controller and perform stability analysis. For large random delay and packet loss, it can be seen from the simulation results that the proposed network control system can reduce the vibration of the offshore platform with a small control force. Compared to other vibrators, paper controllers are more efficient.

The structure of this document is as follows. First, fuzzy TS is briefly considered and a description of the system is presented. Then a set of distributed fuzzy controllers using Parallel Distributed Compensation (PDC) technique is described, and a robust fuzzy control scheme is proposed to overcome the effects of modeling errors. A stability criterion is then provided to guarantee the asymptotic stability of large-scale nonlinear systems with multiple delays. Then a design algorithm is proposed. Finally, a numerical example with simulations is provided to illustrate the results and draw conclusions.

2. System description

This paper studies a networked active vibration controller suitable for agricultural and water engineering. First, let's take a look at peer-to-peer control of a steel marine platform with an AMD device. The scheme of the combined system is shown in the Fig. 1 (see Lu *et al*. 2022) and see more details). Here, the platform can be modeled as a single degree of freedom (SDOF) system, as the first mode affects more dynamic motion. This estimate is sufficient for vibration control.

The modal mass, natural frequency and damping rate of the one-degree-of-freedom (SDOF) system are represented by m_1, respectively, and the μ_1 corresponding x_1 modal coordinates are related to the motion of the ocean platform. The mass, natural frequency, and damping ratio of the m_2 author's AMD device x_1 are denoted by μ_2, respectively, and the x_2 AMD device offset is denoted by x_2. The steering force and the irregular wave force are respectively μ and f. Through physical analysis, we obtain the motion of the coupled system, which is described by the following coupled differential equation.

$$\begin{aligned}\ddot{x_1}(t) = &-\left(\omega_1^2 + \frac{\omega_2^2 m_2}{m_1}\right)x_1(t) + \left(\frac{\omega_2^2 m_2}{m_1}\right)x_2(t)\\ &-2\left(\xi_1\omega_1 + \frac{\xi_2\omega_2 m_2}{m_1}\right)\dot{x_1}(t)\\ &+2\left(\frac{\xi_2\omega_2 m_2}{m_1}\right)\dot{x_2}(t) + \frac{1}{m_1\big(f(t)-u(t)\big)},\\ \ddot{x_2}(t) = &\ \omega_2^2\big(x_1(t)-x_2(t)\big) + 2\xi_2\omega_2\big(\dot{x_1}(t)-\dot{x_2}(t)\big)\\ &+u(t)/m_2\end{aligned}$$

Second, we introduce the network into the control system. Latency, packet loss, and interference inevitably affect system performance and must be carefully considered when modeling and designing controllers.

In Fig. 1, the sensors, controllers and actuators are separated, which means that the front channel (controller to actuator) and the rear channel (sensor to controller) are connected to the network. In this way, distributed sampling and computation can be done throughout the cycle. Grey system theory (Peng and Dong 2011, Sie *et al*. 2006, Truong and Ahn 2012) is used to generate grey models that

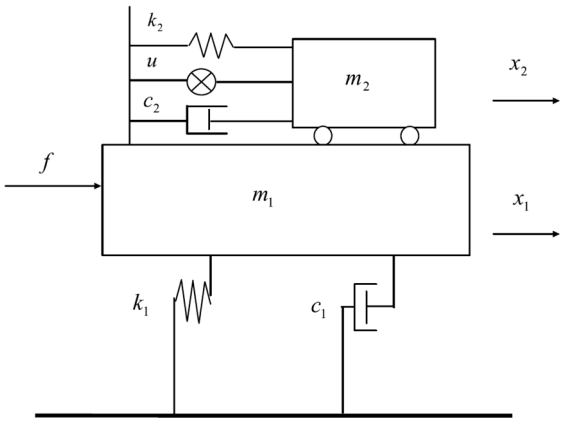

Fig. 1 AMD platform system diagram

can be applied to all control systems. Predict system fluctuations before the current time. The general form of the gray model is the order of the ordinary differential equation of the gray model and the number of gray variables. Building a grey model requires computation time; however, the computation time required grows exponentially with the order of the ordinary differential equations of the Grey model and the number of Grey variables. The GM(1,1) model is one of the gray models and is widely used in control systems to predict system performance because of its faster computational performance than other gray models (see Shi *et al*. 2021, Wang and Li 2021, Quartey-Papafio *et al*. 2021, Li *et al*. 2002 and refs).

The cumulative production function (AGO) can be described as follows

$$\theta^{(1)}(k) = \sum_{\chi=1}^{k} \theta^{(0)}(\chi),$$

where θ represents the build order of the accumulated data, monotonically increasing; χ is an index from 1 to K. θ It is not always a positive data production sequence, such as that derived from the systematic output error at each sampling interval. Therefore, this study uses linear mapping methods (Ma and Xu 2023) to transform their behaviors and obtain positive data generation sequences before proceeding with data generation.

The Inverse Cumulative Generating Operation (IAGO) can be described as (Zhang *et al*. 2017, Ma and Xu 2023, Sie *et al*. 2006)

$$\theta^{(0)}(k) = \theta^{(1)}(k) - \theta^{(1)}(k-1)$$

which the $\theta^{(0)}(k)$ accumulated information is generated is reversed $\theta^{(1)}(k)$.

1) We can form the first-order ordinary differential equation of the model (Zhang *et al*. 2017, Sie *et al*. 2006)

Which

$$\frac{d\theta^{(1)}}{dt} + \mu\theta^{(1)} = v,$$

$\theta^{(1)}$ It can be described as a discrete timeline (Zhang *et al*. 2017, Sie *et al*. 2006).

$$\frac{d\theta^{(1)}}{dt} = \theta^{(1)}(k+1) - \theta^{(1)}(k) = \theta^{(0)}(\mathrm{k+1})$$

and_ v _μ It can be determined and described using the least squares method (Zhang *et al*. 2017, Sie *et al*. 2006)

$$\hat{\varphi} = \binom{\mu}{v} = (\phi^T\phi)^{-1}\phi^T\theta_N$$

Arrays θ_N and ϕ in can be extended and described by name

$$\theta_N = \left[\theta^{(0)}(1)\theta^{(0)}(2)\ldots\theta^{(0)}(N)\right]^T$$

$$\phi = \begin{pmatrix} -\frac{1}{2}(\theta^{(1)}(0) + \theta^{(1)}(1)) & 1 \\ -\frac{1}{2}(\theta^{(1)}(1) + \theta^{(1)}(2)) & 1 \\ \vdots & \vdots \\ -\frac{1}{2}(\theta^{(1)}(N-1) + \theta^{(1)}(N)) & 1 \end{pmatrix},$$

where *N* is the number of datasets used to estimate the Gray parameters. The discrete-time solution can be described as (Zhang *et al*. 2017, Chen 2014b, Sie *et al*. 2006) which

$$\hat{\theta}^{(1)}(k) = \left(\theta^{(1)}(0) - \frac{v}{\mu}\right)e^{-\mu(k-1)} + \frac{v}{\mu}$$

how $\theta^{(1)}(0)$ Defined as follows $\theta^{(0)}(1)$ (Zhang *et al*. 2017, Sie *et al*. 2006), the k+1 stage can be described as follows

$$\hat{\theta}^{(1)}(k+1) = \left(\theta^{(0)}(1) - \frac{v}{\mu}\right)e^{-\mu k} + \frac{v}{\mu}$$

This study can evaluate the prediction dataset in step k+1 as

$$\hat{\theta}^{(0)}(k+1) = \hat{\theta}^{(1)}(k+1) - \hat{\theta}^{(1)}(k)$$

Building a GM(1,1) model to produce reasonably accurate predictions requires at least four sets of data. In this study, five datasets were then selected to form a predictive application in control systems. To clarify the model, we make the following assumptions.

Assumption 1. The sensor-controller and controller-actuator delays can be longer than the sampling period T, and the delays in the rest of the transmission path can be ignored.

Consider a nonlinear decoupling method as follows

$$N_j: \begin{cases} \dot{x}_j(t) = \psi_j(x_j(t), u_j(t)) + \sum_{k=1}^{N_j} g_{kj}(x_j(t-\tau_{kj})) + \varphi_j(t) & \text{(1a)} \\ \varphi_j(t) = \sum_{\substack{n=1 \\ n\neq j}}^{J} C_{nj}x_n(t), & \text{(1b)} \end{cases}$$

where $\psi_j(\cdot)$ and $g_{\overleftrightarrow{k}\overleftrightarrow{j}}(\cdot)$ is the nonlinear vector function $x_j(t)$, $x_j(t-\tau_{\overleftrightarrow{\overleftrightarrow{k}}\overleftrightarrow{j}})$ is the state vector, $\tau_{k\overleftrightarrow{\overleftrightarrow{j}}}$ is the time delay, $u_j(t)$ is the input vector, and is the coupling matrix between the C_{nj} nth subsystem and the *jth subsystem*.

In just over a decade, the locally linear input/output relationship of nonlinear systems using fuzzy dynamical models has been greatly improved in the pioneering work of Takagi and Sugeno (Lu *et al*. 2022). Therefore, *the j-th isolated* (*homogeneous*) *subsystem* ***of N is*** approximated by a multi-delay fuzzy TS model described by the IF-THEN

fuzzy rule. The main feature of the fuzzy TS model is *that each rule is represented by a linear equation of state and rule i*: has the following form (Procyk and Mamdani 1979)

set *to* : yes $x_{1j}(t)$ is M_{i1j} and $\cdots$ and $x_{\eta\, j}(t)$ is $M_{i\eta\, j}$

Interest

$$\dot{x}_j(t) = A_{ij}x_j(t) + \sum_{k=1}^{N_j} A_{ikj}x_j(t-\tau_{kj}) + B_{ij}u_j(t) \qquad (2)$$

where $x_j^T(t) = \left[x_{1j}(t), x_{2j}(t), \cdots, x_{\eta\, j}(t)\right]$, $u_j^T(t) = [u_{1j}(t), u_{2j}(t), \cdots, u_{mj}(t)]$.

$i = 1, 2, \cdots, r_j$ y r_j is the number of IF-THEN rules. A_{ij}, $A_{i\rightrightarrows k\rightrightarrows j}$ and B_{ij} are two appropriately sized arrays, and M_{ipj} $(p = 1, 2, \cdots, \eta)$ are fuzzy sets and $x_{1j}(t) \sim x_{\eta j}(t)$ standard variables. The final state of this dynamic fuzzy model is derived as follows

$$\dot{x}_j(t) = \frac{\sum_{i=1}^{r_j} w_{ij}(t)[A_{ij}x_j(t) + \sum_{k=1}^{N_j} A_{ikj}x_j(t-\tau_{kj}) + B_{ij}u_j(t)]}{\sum_{i=1}^{r_j} w_{ij}(t) = \sum_{i=1}^{r_j} h_{i\rightrightarrows j}(t)[A_{i\rightrightarrows j}x_j(t) + \sum_{k=1}^{N_j} A_{i\rightrightarrows k\rightrightarrows j}x_j(t-\tau_{kj}) + B_{i\rightrightarrows j}u_j(t)]} \qquad (3)$$

and

$$w_{ij}(t) = \prod_{p=1}^{\eta} M_{ipj}\left(x_{pj}(t)\right), \qquad h_{ij}(t) = \frac{w_{ij}(t)}{\sum_{i=1}^{r_j} w_{ij}(t)} \qquad (4)$$

with $M_{ipj}(x_{pj}(t))$ belong $x_{pj}(t)$. This M_{ipj} article assumes $w_{ij}(t) \geq 0$, $i = 1, 2, \cdots, r_j$, for $\sum_{i=1}^{r_j} w_{ij}(t) > 0$ all *t*. Where $h_{ij}(t) \geq 0$, $i = 1, 2, \cdots, r_j$ for $\sum_{i=1}^{r_j} h_{ij}(t) = 1$ all *t*. Hence the Eq. (1) We have

$$N_j: \begin{cases} \dot{x}_j(t) = \sum_{i=1}^{r_j} h_{ij}(t)(A_{ij}x_j(t) + B_{ij}u_j(t) + \sum_{k=1}^{N_j} A_{ikj}x_j(t-\tau_{kj})) + [\psi_j(x_j(t), u_j(t)) + \sum_{k=1}^{N_j} g_{kj}(x_j(t-\tau_{kj})) \\ \qquad - \sum_{i=1}^{r_j} h_{ij}(t)(A_{ij}x_j(t) + B_{ij}u_j(t)) - \sum_{i=1}^{r_j}\sum_{k=1}^{N_j} h_{ij}(t)(A_{ikj}x_j(t-\tau_{kj}))] + \varphi_j(t) \\ \varphi_j(t) = \sum_{\substack{n=1 \\ n\neq j}}^{J} C_{nj}x_n(t) \end{cases} \qquad (5)$$

In the next section, the PDC model is used for fuzzy controller design.

3. Diffuse linear differential neuronal Inclusions

A neural network based model can be described as follows

$$\dot{x}_j(t) = A_{ij}x_j(t) + \sum_{k=1}^{N_j} A_{ikj}x_j\left(t-\tau_{kj}\right) + B_{ij}u_j(t), \qquad (6)$$

where $\Lambda^T(t) = [X^T(t) \quad U^T(t)]$, with $X^T(t) = [x_1(t) \quad x_2(t) \quad \Lambda \quad x_\delta(t)]$. Suppose the S layers and each layer have $R^\sigma(\sigma = 1,2,\Lambda,S)$ neurons, where $x_1(t) \sim x_\delta(t)$ sum $u_1(t) \sim u_m(t)$ is the input variable. This notation W^σ gives the weight matrix σ^{th} $(\sigma = 1,2,\cdots,S)$ apartment. The layer transfer function vector $\sigma^{th}$is defined as $\psi^\sigma(v) = [T(v_1) \quad T(v_2) \quad \ldots \quad T(v_{R^\sigma})]^T$.

NNDI systems can be described by spatial representations as follows

$$\dot{Y}(t) = A(a(t))Y(t), A(a(t)) = \sum_{i=1}^{r} h_i\,(a(t))\bar{A}_i,$$

where r is a positive integer; $a(t)$ is a vector representing the dependencies of its elements $h_i(g)$, $a(t) = [a_1(t), a_2(t), L, a_n(t)]^T$ i.e., $h_i\left(a(t)\right) \equiv h_i(a_1(t), a_2(t), L, a_n(t))$ (usually, $a(t)$ Affect state vector $X(t)$); $\bar{A}_i(i = 1,2,\Lambda,r)$ is a constant matrix; and $Y(t) = [y_1(t) \quad y_2(t) \quad \Lambda \quad y_j(t)]^T$.

After the interpolation process, we have

$$\dot{X}(t) = \left[\sum_{\zeta^S=1}^{2} h_{\zeta^S}(t)G_\zeta^S\left(W^S\left[\cdots\left[\sum_{\zeta^2=1}^{2} h_{\zeta^2}(t)G_\zeta^2\left(W^2\left[\sum_{\zeta^1=1}^{2} h_{\zeta^1}(t)G_\zeta^1\left(W^1\Lambda(t)\right)\right]\right)\right]\Lambda\right]\right)\right]$$
$$= \sum_{\zeta^S=1}^{2}\Lambda\sum_{\zeta^2=1}^{2}\sum_{\zeta^1=1}^{2} h_{\zeta^S}(t)\Lambda\, h_{\zeta^2}(t)h_{\zeta^1}(t)G_\zeta^S W^S\Lambda G_\zeta^2 W^2 G_\zeta^1 W^1\Lambda(t) = \sum_{\Omega^\delta} h_{\Omega^\delta}(t)E_{\Omega^\delta}\Lambda(t) \qquad (7)$$

Where $\sum_{\zeta^\delta} h_{\zeta^\delta}(t) = \sum_{q_1^\sigma=1}^{2} \sum_{q_2^\sigma}^{2} \cdots \sum_{q_{R^\sigma}^\sigma=1}^{2} h_{q_1^\sigma}(t)$ $h_{q_2^\sigma}(t) \cdots h_{q_{R^\sigma}^\sigma}(t)$ be opposed to $\sigma = 1,2,\Lambda,S$; $h_{q_\varsigma^\sigma}(t) \in [0,1]$, $\sum_{q_\varsigma^\sigma=1}^{2} h_{q_\varsigma^\sigma}^{\sigma}(t) = 1$ be opposed to $\varsigma = 1,2,\Lambda,$ R^σ; $E_{\Omega^\sigma} \equiv G_\varsigma^S W^S \cdots G_\varsigma^2 W^2 G_\varsigma^1 W^1$; $\dot{x}_j(t) = A_{i\rightleftarrows j} x_j(t) +$ $\sum_{k=1}^{N_j} A_{i\rightleftarrows k\rightleftarrows j} x_j(t-\tau_{k\rightleftarrows j}) + B_{i\rightleftarrows j} u_j(t)$

Finally, based on the Eq. (7), the dynamics of the NN model can be rewritten as NNDI

$$\dot{X}(t) = \sum_{i=1}^{r} h_i(t) E_i \Lambda(t), \tag{8}$$

where $h_i(t) \geq 0$; $\sum_{i=1}^{r} h_i(t) = 1$; $r$is a positive integer; y $\bar{E}_i$ is a constant array associated with the appropriate dimension E_{Ω^σ} The representation of NNDI can be rearranged as follows

$$\dot{X}(t) = \sum_{i=1}^{r} h_i(t)\{A_i X(t)\}, \tag{9}$$

Where A_i is the partition E_i corresponding to the partition $\Lambda(t)$

Based on the model diagram of the NN-based method described above, the nonlinear system can be approximated by the NNDI representation (9). this The NNDI representation follows the same rules as the TS model for fuzzy machine learning, combining the flexibility of fuzzy logic machine learning theory and the rigorous mathematical analysis tools of linear systems theory into a unified framework. To ensure the stability of the TLP system, return to the TS machine learning model and stability analysis. First, the *rule i*: *representing* the TS fuzzy machine learning model of the structural system *can be expressed as*

Rule i : IF $x_1(t)$ is $M_{i1}$and Λ e $x_p(t)$ is M_{ip},

Intellectual Property

$$\dot{x}_j(t) = A_{ij} x_j(t) + \sum_{k=1}^{N_j} A_{ikj}\, x_j(t-\tau_{kj}) + B_{ij} u_j(t) \tag{10}$$

where $i = 1,2,\Lambda,r$ y r is the rule number; $X(t)$ is the state vector; M_{ip} $(p = 1,2,\Lambda,g)$ They are fuzzy sets of machine learning and $x_1(t) \sim x_p(t)$ standard variables. Using a machine learning fuzzy inference method with eleven fuzzers, a product inference, and an average defuzzer, a dynamic machine learning fuzzer Model can express.

4. Fuzzy control design

Subsequently, a stability criterion is proposed to guarantee ***the asymptotic stability of large nonlinear multi-relay N systems.*** Before considering asymptotic stability, the following is a useful concept.

Lemma 1 (Peng and Dong, 2011)**: For all** appropriately sized *X and Y matrices*

$$X^T Y + Y^T X \leq \xi \rightleftarrows X^T X + \xi^{-1} Y^T Y \tag{11}$$

where ξ is a normal number.

Theorem 1: Large nonlinear systems *with multiple delays* N are If it is a positive constant, it is asymptotically stable β, α_j and κ_j has ρ_j, $j = 1, 2, \cdots, J$ and get feedback $K_{i\rightleftarrows j}$ to be selected as satisfied

(1)

$$\bar{\lambda}_j \equiv \max_k \lambda_M\left(\bar{Q}_{k\rightleftarrows j}\right) < 0 \quad (k = 1, 2, \cdots, N_j) \tag{12a}$$

$$\lambda_{ij} \equiv \lambda_m\left(Q_{ij}\right) > 0 \quad \text{to} \quad i = 1, 2, \cdots, r_j \tag{12b}$$

$$\lambda_{\rightleftarrows i\rightleftarrows f\rightleftarrows\rightleftarrows j} \equiv \lambda_m\left(Q_{i\rightleftarrows f\rightleftarrows j\rightleftarrows}\right) > 0 \quad \text{to} \quad i < f \leq r_j \tag{12c}$$

Where

(2)

$$\Lambda_j \equiv \begin{bmatrix} -\bar{\lambda}_j & 0 & 0 & \cdots & 0 \\ 0 & \lambda_{1j} & \dfrac{1}{2\lambda_{12j}} & \cdots & \dfrac{1}{2\lambda_{1r_jj}} \\ 0 & 1/2\lambda_{12j} & \lambda_{2j} & \cdots & \dfrac{1}{2\lambda_{2r_jj}} \\ \vdots & \vdots & \vdots & \ddots & \vdots \\ 0 & 1/2\lambda_{1r_jj} & \dfrac{1}{2\lambda_{2r_jj}} & \cdots & \lambda_{r_jj} \end{bmatrix} > 0, \tag{13}$$

and $\lambda_M(\bar{Q}_{k\rightleftarrows j})$ represent the largest eigenvalue $\bar{Q}_{k\rightleftarrows j}$. In addition $\lambda_m(Q_{i\rightleftarrows j})$ and $\lambda_m(Q_{i\,f\,j})$ respectively denote $Q_{i\rightleftarrows j}$ eigenvalues less than $Q_{i\,f\,j}$.

Certificate: see attachment.

Note 1 (Truong and Ahn 2012) : Basically, two terms in an Eqs. (12) and (13) can be used to test the asymptotic stability of ***N*** multi-delay large nonlinear systems. So, it makes sense to test for asymptotic stability under these two conditions, and return the other condition if it fails.

5. Algorithms

The whole design process can be summarized as the following algorithm.

***Offshore platform vibration for a* large** nonlinear multi-delay system using the Lyapunov stability criterion.

The above problem can be solved by the following steps.

Step 1: Select fuzzy factory rules and membership functions as inputs to the TS fuzzy model for each nonlinear subsystem to be generated.

Step 2: Synthesize a series of fuzzy distributed controllers using the PDC model concept.

Step 3: From observation 1, choose the limit matrix $\Delta H_{ifj}(=\delta_{ifj}H_{qj})$ sum to $j = 1, 2, \cdots, J$ satisfy $k = 1, 2, \cdots, N_j$ equation $\Delta H_{ikj}(=\delta_{ikj}\bar{H}_{qj})$ (4.1.4) and equation. $i, f = 1, 2, \cdots, r_j$ (4.1.5) or

Step 4: If P_j there is a positive definite matrix output and, in order to satisfy one of the stability conditions in

Theorem 1, based on the control model synthesized in Step 2, the $R_{k\rightleftarrows j}$ ***large-scale nonlinear multi-delay system N*** can be asymptotically stabilized by the nebula. $k = 1, 2, \cdots, N_j$, Repeat steps 2 and 3 to find $\Delta H_{i\,k\,j}$ a suitable fuzzy control and contour matrix $\Delta H_{i\,f\,j}$ that satisfies either condition (I) or condition (II).

(EBA) is proposed based on the complex system of extensive echolocation of bats in nature. Unlike other swarm sub-algorithms, EBA has the advantage that only one parameter called support needs to be determined before using the algorithm for troubleshooting. The choice of different tools determines the dimension of another research stage in the evolutionary process. In this study, we chose air as the environment because it is the main environment in which bats live. The functions of ABE can be summarized as follows.

Initialization: Artificial means are distributed in the solution space receiving random coordinates.

Movement: The movement of man-made objects. Generate a random number and check if it is greater than a fixed ping rate. If the result is positive, the human agent moves in a random walk method.

$x_i^t = x_i^{t-1} + D$, where represents the coordinates of the x_i^t ith human agent in the t-th iteration, represents the coordinates of the x_i^{t-1} ith human agent in the last iteration, and D is the distance traveled by the human agent in this iteration.

$D = \gamma \cdot \Delta T$, the constant corresponds $\gamma$to the medium chosen in the experiment and $\Delta T \in [-1,1]$ is a random number. $\gamma = 0.17$. It was used in our experiments because the medium of choice was air.

$$x_i^{tR} = \beta(x_{best} - x_i^t), \quad \beta \in [0,1]$$

There is β a random number; x_{best} the coordinates that provide the best solution found so far in all artificial matter; y x_i^{tR} represents the new coordinates artificially averaged through a random walk process.

Evaluation: The suitability of plastics is calculated and updated to the optimal storage solution using a custom suitability function. The flow chart of the algorithm used in the optimization is shown in Fig. 1. That is, the input and output responses of the system are estimated using the grey prediction algorithm described above. Therefore, the input variable of the FLC plant related to the expected output response of the system via GM(1,1) will be $\hat{\theta}_{yi}^{(0)}(k+1)$. Fuzzy logic control variables is described as

$$\begin{aligned}
&\hat{e}_i(k+1) = \theta_{ri}(k+1) - \hat{\theta}_{yi}^{(0)}(k+1);\\
&\hat{ec}_i(k+1) = \hat{e}_i(k+1) - e_i(k);\\
&e_i(k) = \theta_{ri}(k) - \theta_{yi}(k),\\
&\hat{s}_i(k) = \lambda_i \hat{e}_i(k+1) + \hat{ec}_i(k+1),\\
&\Delta\hat{s}_i(k) = \hat{s}_i(k) - \hat{s}_i(k-1).
\end{aligned}$$

6. Example

In this section, we analyze networked vibration controllers introduced for large shell-type offshore platforms with various delays. First, the parameters of wave structure and strength are described. The effects of delays and interruptions are discussed below. Finally, the performance of the proposed controller is compared with different controllers.

The water structure depth of the offshore platform (Lu *et al*. 2022) is d = 218 m, the total platform height L = 249 m, corresponding to a four-foot characteristic diameter D = 1.83 m, the first modal mass m_1 = 7,825,307 kg, and the platform natural frequency u_1 = 2.0466 rad/s, Structural Damping Coefficient x_1 = 2%. AMD devices are mounted on the chassis screen as shown in Fig. 2. The characteristics of the AMD device are as follows: mass m_2 = 78.253 kg, u_2 natural frequency = 2.0074 rad/s, frame damping ratio x_2 = 20%. Here the sampling period of the discrete time system is T = 0.01 s and we can get the parameters.

$$A = \begin{bmatrix} 0.9998 & 0.0000 & 0.0100 & 0.0000 \\ 0.0002 & 0.9998 & 0.0000 & 0.0100 \\ -0.0423 & 0.0004 & 0.9989 & 0.0001 \\ 0.0400 & -0.0401 & 0.0082 & 0.9918 \end{bmatrix},$$

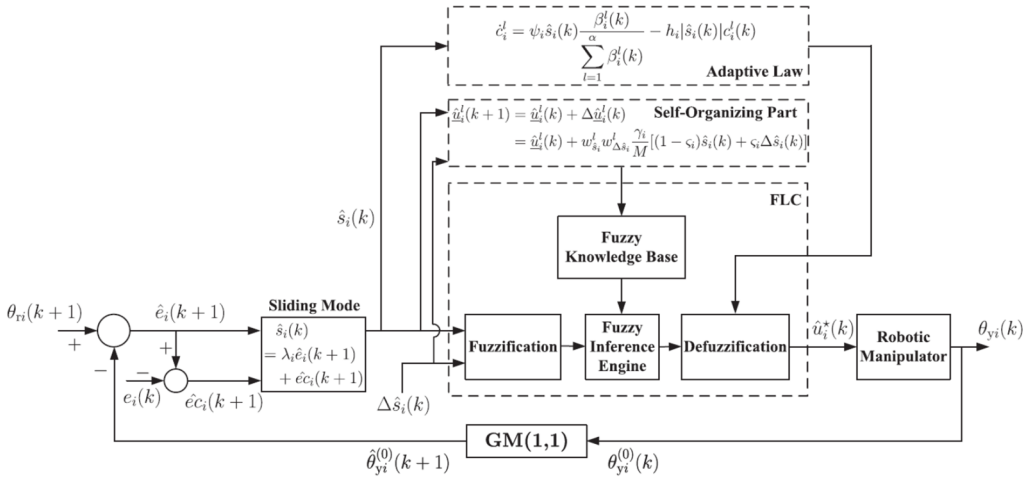

Fig. 2 Flowchart of the coupled system optimization algorithm

$$B = 10^{-6} * \begin{bmatrix} 0.0000 \\ 0.0006 \\ -0.0013 \\ 0.1273 \end{bmatrix}, \quad D = 10^{-8} * \begin{bmatrix} 0.0006 \\ 0.0000 \\ 0.1277 \\ 0.0005 \end{bmatrix}$$

where H_s is the effective height of the wave, ω_0 is the peak frequency, is the ω wave frequency, γ is the peak parameter, and $\beta = exp[-(\omega - \omega_0)^2/(2\sigma^2\omega_0^2)]$ is the σ shape parameter $\sigma = 0.07$ $(\omega \leq \omega_0)$. $\sigma = 0.09$ $(\omega > \omega_0)$. Here H_s = 7 m, ω_0 = 0.79 rad/s and γ = 3.3. The power spectral density (PSD) of wave height and intensity are shown in Figs. 3-4. C_m Calculate the wave intensity C_d **f using values = 1.0 and = 1.5.** From point (14), the irregular wave force acting on the ship at sea can be obtained, as shown in Fig. 5. For the vibration control system of the offshore platform network of performance index (20), we set $\mathbf{Q} = 10^7 * diag(1 \quad 0 \quad 1 \quad 0)$. $\mathbf{R} = 10^{-5}$, N = 210/T.

As shown in figure, the network between distributed equipment and offshore platforms distinguishes NCS from traditional point-to-point control systems. Due to the harsh environment, delay and packet loss are unavoidable most of the time. In this section, we describe the packet loss for two independent Bernoulli processes (sensor-controller and controller-actor). If a packet from the sensor to the controller is lost, the random variable $d^{sc}(k)$ has a probability of getting the value 1. A random variable $\mu_1$may get a value of 1 μ_2 if packets from the controller to the actuator are lost $d^{ca}(k)$.

In this subsection, we analyze the performance of drivers with different latency and packet loss rates. In a networked control system (Zhang *et al.* 2014), the upper bound of the delay is assumed to be m ^{sc} = 0.7 / T = 70 at ^{ca} = 0.7 / T = 70. So, M = 140, which is a big delay nod. With the above parameters, we get the following $\boldsymbol{m_1}$ simulation results for different sums of packet loss rates $\boldsymbol{m_2}$. It shows the displacement and acceleration of the offshore platform under different bag falling speeds. In the stability criteria, the control force to damping ratios 0, 02, 0.05 and 1.0 are used in and plotted in Figs. 6-7. Furthermore, Theorem 1 can be used to guarantee the stability of multiple timers. The large system and this case of a shell-shaped offshore platform proved feasible and stable, obtaining the following parameters.

$$P_1 = \begin{bmatrix} 2.7632 & -1.0422 \\ -1.0422 & 2.6941 \end{bmatrix},$$
$$P_2 = \begin{bmatrix} 1.2935 & 0.0604 \\ 0.0604 & 0.7923 \end{bmatrix},$$
$$R_{23} = \begin{bmatrix} 0.73 & 0 \\ 0 & 0.73 \end{bmatrix}, \quad R_{13} = \begin{bmatrix} 0.6 & 0 \\ 0 & 4.4 \end{bmatrix}$$
$$P_3 = \begin{bmatrix} 1.2671 & 0.0244 \\ 0.0244 & 2.0531 \end{bmatrix},$$
$$R_{11} = \begin{bmatrix} 3 & -2.6 \\ -2.6 & 4.5 \end{bmatrix}, \quad R_{21} = \begin{bmatrix} 3 & -0.6 \\ -0.6 & 4.5 \end{bmatrix}$$
$$R_{12} = \begin{bmatrix} 3.7 & 2 \\ 2 & 3.7 \end{bmatrix}, \quad R_{22} = \begin{bmatrix} 2 & 0 \\ 0 & 2 \end{bmatrix}$$

with $\rho_1 = 1,\ \rho_2 = 1, \rho_3 = 1,\ \kappa_1 = 10,\ \kappa_2 = 2,\ \kappa_3 = 14,$ $\alpha_1 = 1.8,\ \alpha_2 = 1,\ \alpha_3 = 6.5.$

For fixed delay and variable packet loss rate, our results allow us to study the impact of packet loss rate on system performance. On the other hand, for fixed packet loss rate and variable delay ^{mca} or ^{msc}, the effect of delay and packet loss rate on system performance can be studied.

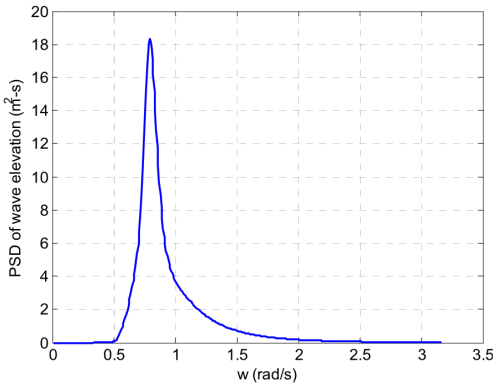

Fig. 3 PSD wave height

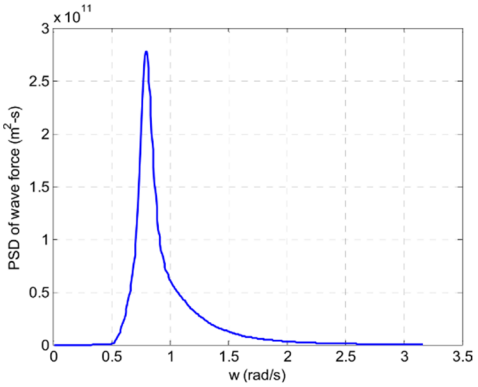

Fig. 4 Wave power DSP

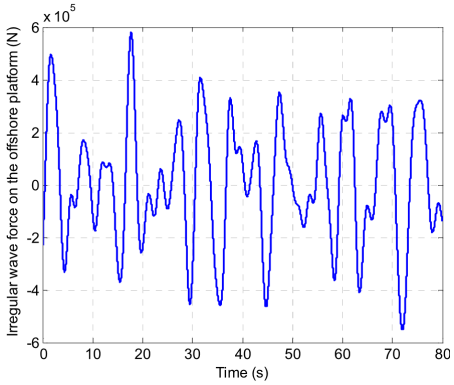

Fig. 5 Irregular wave forces impact offshore structures

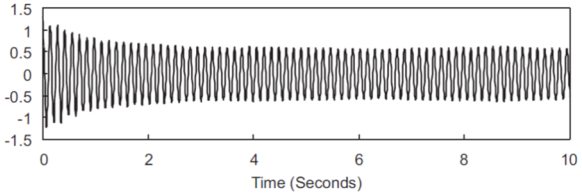

Fig. 6 Offshore mobile platforms

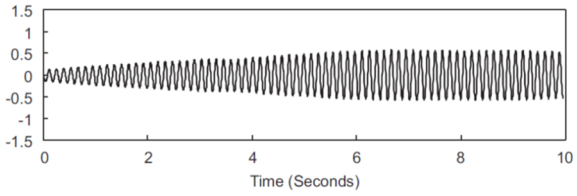

Fig. 7 The offshore platform accelerates

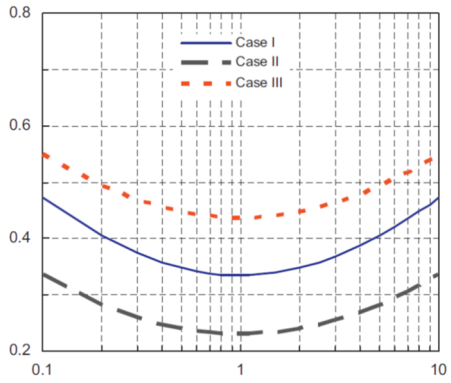

Fig. 8 The driving force affects the amplitude at different damping rates

As the packet loss rate increases, more and more control signals are lost in the network transmission, so the actuatoroutput must use the previous control force value more frequently. When $\boldsymbol{d^{ca}(k) = 1}$ we $\boldsymbol{\bar{u}(k) = \bar{u}(k-1)}$ have it means that the system process usually doesn't have the power to check the current state. At the same time, separation becomes violent. The asynchronous phenomenon reduces the system performance, increases the displacement and acceleration of the offshore platform, and has a high packet loss rate. after Vibrations in the high seas became violent. To reduce structural vibrations, the maximum drive force and actuator power have also been increased. In $\boldsymbol{m_1}$ the case of ¼ ¼, 100% equals no control $\boldsymbol{m_2}$.

Fig. 8 shows the error detection history of the learning process using Single Input Single Output Fuzzy Control (SOFC), Grey Predictive SOFC (GPSOFC) and Grey Advanced Predictive SOFC (EAGSFSC) to detect link states. Route planning motion control. Note that using SOFC requires four learning cycles to achieve reasonable performance; however, using GPSOFC or EAGSFSC alone requires only two learning cycles. Desired path (reference input) and output response They are too close to distinguish. Further comparison of steering performance These controls, Figs. 9(b) and 9(c) show the paths after control failure and overload, respectively. It can be seen that the maximum path (absolute value) and root mean square (RMS) after SOFC failure are around 0.1583 and 0.0305, respectively; however, for GPSOFC, the above errors have been reduced to around 0.0810 and 0.0198, and for EAGSFSC, the above errors have been reduced to about 0.0331 and 0.0010. Fig. 9(c) shows that the control of EAGSSFSC is easier than that of GPSOFC and SOFC. This means that the lifespan of the robot controlled by EAGSFSC will be longer than that of GPSOFC and SOFC can be seen in the figure. From Fig. 9, it can be seen that GPSOFC achieves better control performance than SOFC in motion control trajectory planning because it applies Gray GM(1,1) prediction algorithm in SOFC to eliminate the problem of wrong selection. parameters in SOFC and compensate for dynamic coupling effects between robot degrees of freedom. The required learning period for GPSOFC is also the same as EAGSFSC for robot path planning, but EAGSFSC performs even better than GPSOFC. Of course, EAGSFSC not only has the original characteristics of GPSOFC, but also has an adaptive law, which can adjust the FLC to a reasonable value for real-time control design. This setting ensures stable system operation and further improves system control performance. This study found that trajectory planning using GPSOFC or EAGSFSC in motion control provides adequate control performance even within two learning cycles. Although GPSOFC and EAGSFSC can still be used to control robotic systems with more than two learning cycles, the control performance of the system is not significantly improved. The performance of the EAGSFSC or GPSOFC control with more than two learning cycles is almost the same as the control with only two learning cycles. In particular, EAGSFSC and GPSOFC are unlikely to improve control performance by adding more learning cycles after reaching reasonable performance.

Fig. 10 shows the comparison between the simulation and experiment that represents the good performance of the simulations. Fig. 11 shows the stretchered control result is better than the one without unstretchered.

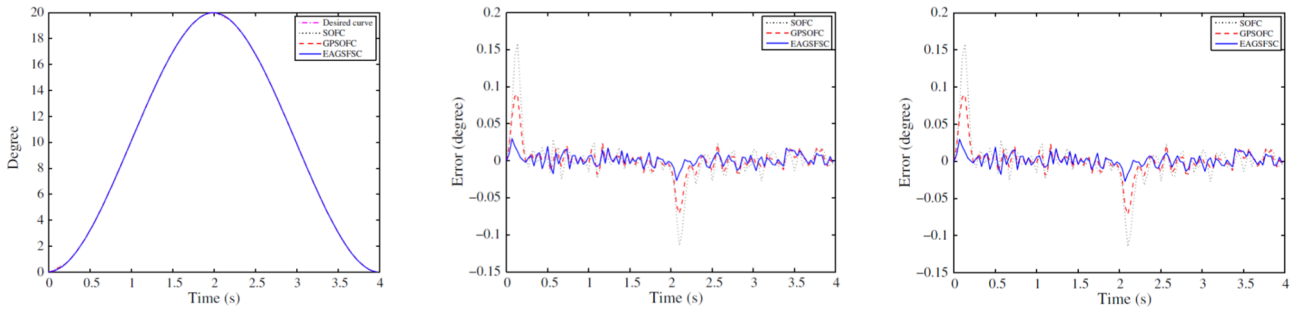

(a) (b) (c)

Fig. 9 Comparison of SOFC, GPSOFC and EAGSFSC orbit planning control performance: (a) orbital tracking response; (b) tracking error; and (c) control voltage

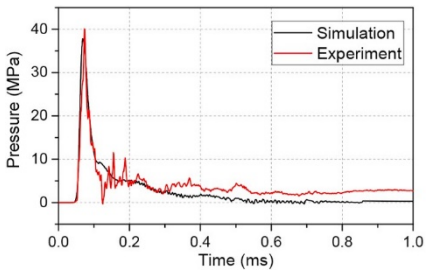

Fig. 10 Comparison of experimental and analytical result

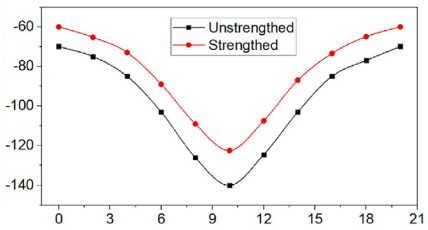

Fig. 11 Performance of the proposed design

7. Conclusions

The article presents the robustness of fuzzy control using a model-based approach. The impact of modeling errors. To ensure the asymptotic stability of large-scale nonlinear multi-delay systems, the stability criterion is derived from the direct Lyapunov method. Based on this criterion and a distributed control system, a set of model-based fuzzy controllers is synthesized to stabilize large-scale nonlinear multi-delay systems. Finally, an example image with simulation is given to illustrate the results.

Acknowledgments

The authors are grateful for the research grants given to Ruei Yuan Wang from GDUPT talent introduction, Peoples R China under Grant No. 702 519208, the Projects of Talents Recruitment of GDUPT (NO. 2019rc098), and the research grants given to ZY Chen from the Projects of Talents Recruitment of GDUPT (NO. 2021rc002) in Guangdong Province, Peoples R China, as well as to the anonymous reviewers for constructive suggestions.

References

Chan, J., Xu, S. and Zhang, B. (2017), "Single/multiple integral inequalities with applications to stability analysis of time-delay systems", *IEEE Transact. Automatic Control*, **62**, 3488-3493. https://doi.org/10.1109/TAC.2016.2617739

Chang, M. (2010), "An adaptive self-organizing fuzzy sliding mode controller for a 2-DOF rehabilitation robot actuated by pneumatic muscle actuators", *Control Eng. Practice*, **18**, 13-22. https://doi.org/10.1016/j.conengprac.2009.08.005

Chen, C. (2014a), "A criterion of robustness intelligent nonlinear control for multiple time-delay systems based on fuzzy Lyapunov methods", *Nonlinear Dyn.*, **76**, 23-31. https://doi.org/10.1007/s11071-013-0869-9

Chen, C. (2014b), "Interconnected TS fuzzy technique for nonlinear time-delay structural systems", *Nonlin. Dyn.*, **76**(1), 13-22. https://doi.org/10.1007/s11071-013-0841-8

Cheng, L., Yin, F., Theodoridis, S., Chatzis, S. and Chang, T. (2022), "Rethinking Bayesian Learning for Data Analysis: The art of prior and inference in sparsity-aware modeling", *IEEE Signal Process. Magaz.*, **39**(6), 18-52. https://doi.org/10.1109/MSP.2022.3198201

Chon, T. (2021), "Smart structural stability and NN based intelligent control for nonlinear systems", *Smart Struct. Syst., Int. J.*, **27**(6), 917-926. https://doi.org/10.12989/sss.2021.27.6.917

Fu, Q., Si, L., Liu, J., Shi, H. and Li, Y. (2022), "Design and experimental study of a polarization imaging optical system for oil spills on sea surfaces", *Appl. Opt.*, **61**(21), 6330-6338. https://doi.org/10.1364/AO.456305

Gu, M., Mo, H., Qiu, J., Yuan, J. and Xia, Q. (2022), "Behavior of floating stone columns reinforced with geogrid encasement in model tests", *Front. Mater.*, **9**, p. 980851. https://doi.org/10.3389/fmats.2022.980851

Han, Y., Xu, X., Zhao, Y., Wang, X., Chen, Z. and Liu, J. (2022a), "Impact of consumer preference on the decision-making of prefabricated building developers", *J. Civil Eng. Manag.*, **28**(3), 166-176. https://doi.org/10.3846/jcem.2022.15777

Han, Y., Yan, X. and Piroozfar, P. (2022b), "An overall review of research on prefabricated construction supply chain management", *Eng. Constr. Architect. Manag.* [ahead-of-print] https://doi.org/10.1108/ECAM-07-2021-0668

Han, Y., Wang, L. and Kang, R. (2023), "Influence of consumer preference and government subsidy on prefabricated building developer's decision-making: a three-stage game model", *J. Civil Eng. Manag.*, **29**(1), 35-49. https://doi.org/10.3846/jcem.2023.18038

Hasan, S.D., Islam, N. and Moin, K. (2010), "A review of fixed offshore platforms under earthquake forces", *Struct. Eng. Mech., Int. J.*, **35**, 479-491. https://doi.org/10.12989/sem.2010.35.4.479

Hsu, W., Yang, R., Chang, F., Wu, H. and Chen, H. (2015), "Experimental study of floating offshore platform in combined wind/wave/current environment", *Int. J. Offshore Polar Eng.*, **26**, 125-131. https://doi.org/10.17736/ijope.2016.mmr13

Hu, Y., Jiang, P., Jiang, H. and Tsai, J. (2021), "Bankruptcy prediction using multivariate grey prediction models", *Grey Syst. Theory Appl.*, **11**, 46-62. https://doi.org/10.1108/GS-12-2019-0067

Huang, H., Huang, M., Zhang, W. and Yang, S. (2020), "Experimental study of predamaged columns strengthened by HPFL and BSP under combined load cases", *Struct. Infrastr. Eng.*, **17**(9), 1210-1227. https://doi.org/10.1080/15732479.2020.1801768

Li, S. and Geng, Z. (2023), "Bicriteria scheduling on an unbounded parallel-batch machine for minimizing makespan and maximum cost", *Inform Process. Lett.*, **180**, 106343. https://doi.org/10.1016/j.ipl.2022.106343

Li, H.J., Wang, S.Q. and Ji, C.Y. (2002), "Semi-active control of wave-induced vibration for offshore platforms by use of MR damper", *China Ocean Eng.*, **16**, 33-40.

Li, J., Xu, K., Chaudhuri, S., Yumer, E., Zhang, H. and Guibas, L. (2017), "GRASS: generative recursive autoencoders for shape structures", *ACM Transact. Graphics*, **36**(4), 1-14. https://doi.org/10.1145/3072959.3073637

Li, D., Yu, H., Tee, K.P., Wu, Y., Ge, S.S. and Lee, T.H. (2021), "On time-synchronized stability and control", *IEEE Transact. Syst. Man Cybernet.: Syst.*, **52**(4), 2450-2463. https://doi.org/10.1109/TSMC.2021.3050183

Lu, S., Ban, Y., Zhang, X., Yang, B., Yin, L., Liu, S. and Zheng, W. (2022), "Adaptive control of time delay teleoperation system

with uncertain dynamics", *Front. Neurorobot*., **16**, 928863. https://doi.org/10.3389/fnbot.2022.928863
Ma, Q. and Xu, S. (2023), "Intentional delay can benefit consensus of second-order multi-agent systems", *Automatica*, **147**, 110750. https://doi.org/10.1016/j.automatica.2022.110750
Ma, H., Tang, G. and Hu, W. (2009), "Feedforward and feedback optimal control with memory for offshore platforms under irregular wave forces", *J. Sound Vib*., **328**, 369-381. https://doi.org/10.1016/j.jsv.2009.08.025
Patil, K. and Jangid, R.S. (2005), "Passive control of offshore jacket platforms", *Ocean Eng*., **32**, 1933-1949. https://doi.org/10.1016/j.oceaneng.2005.01.002
Peng, Y. and Dong, M. (2011), "A hybrid approach of HMM and grey model for age-dependent health prediction of engineering assets", *Expert Syst*. *Appl*., **38**, 12946-12953. https://doi.org/10.1016/j.eswa.2011.04.091
Procyk, T.J. and Mamdani, E. (1979), "A linguistic self-organizing process controller", *Autom*., **15**, 15-30. https://doi.org/10.1016/0005-1098(79)90084-0
Quartey-Papafio, T.K., Javed, S.A. and Liu, S. (2021), "Forecasting cocoa production of six major producers through ARIMA and grey models", *Grey Syst*.: *Theory Applicat*., **11**(3), 434-462. https://doi.org/10.1108/GS-04-2020-0050
Sakthivel, R., Santra, S., Mathiyalagan, K. and Anthoni, S. (2014), "Robust reliable sampled-data control for offshore steel jacket platforms with nonlinear perturbations", *Nonlinear Dyn*., **78**, 1109-1123. https://doi.org/10.1007/s11071-014-1500-4
Shen, X., Yue, M., Duan, P., Wu, G. and Tan, X. (2019), "Application of grey prediction model to the prediction of medical consumables consumption", *Grey Syst*. *Theory Appl*., **9**, 213-223. https://doi.org/10.1108/GS-11-2018-0059
Shi, J., Xiong, P., Yang, Y. and Quan, B. (2021), "Forecasting smog in Beijing using a novel time-lag GM (1,N) model based on interval grey number sequences", *Grey Syst*. *Theory Appl*., **11**(4), 754-778. https://doi.org/10.1108/GS-02-2020-0025
Sie, W., Lian, R. and Lin, B. (2006), "Enhancing grey prediction fuzzy controller for active suspension systems", *Vehicle Syst*. *Dyn*., **44**, 407-423. https://doi.org/10.1080/00423110500320425
Sun, R., Wang, J., Cheng, Q., Mao, Y. and Ochieng, W.Y. (2021), "A new IMU-aided multiple GNSS fault detection and exclusion algorithm for integrated navigation in urban environments", *GPS Solut.*, **25**(4), 1-17. https://doi.org/10.1007/s10291-021-01181-4
Truong, D. and Ahn, K. (2012), "Wave prediction based on a modified grey model MGM (1, 1) for real-time control of wave energy converters in irregular waves", *Renew*. *Energy*, **43**, 242-255. https://doi.org/10.1016/j.renene.2011.11.047
Tsai, P., Pan, J., Liao, B., Tsai, M. and Istanda, V. (2011), "Bat algorithm inspired algorithm for solving numerical optimization problems", *Appl*. *Mech*. *Mater*., **148-149**, 134-137. https://doi.org/10.4028/www.scientific.net/AMM.148-149.134
Wang, S. and Li, N. (2021), "Semi-active vibration control for offshore platforms based on LQG method", *J. Marine Sci*. *Technol*., **21**, 562-568. https://doi.org/10.6119/JMST-012-0917-2
Wang, S., Yue, Q. and Zhang, D. (2013), "Ice-induced non-structure vibration reduction of jacket platforms with isolation cone system", *Ocean Eng*., **70**, 118-123. https://doi.org/10.1016/j.oceaneng.2013.05.018
Xiao, S., Cao, Y., Wu, G., Guo, Y., Gao, G., Chen, S., Liu, P., Wang, Z., Li, P., Yu, J. and Zhang, Y. (2022), "Influence of the distributed grounding layout for intercity trains on the 'train-rail' circumflux", *IEEE Transact. Circuits Syst. II: Express Briefs*. https://doi.org/10.1109/TCSII.2022.3223984
Xu, W., Qu, S. and Zhang, C. (2022), "Fast terminal sliding mode current control with adaptive extended state disturbance observer for PMSM system", *IEEE J. Emerg. Select. Topics Power Electron*. https://doi.org/10.1109/JESTPE.2022.3185777
Xu, S., Dai, H., Feng, L., Chen, H., Chai, Y. and Zheng, W.X. (2023), "Fault Estimation for Switched Interconnected Nonlinear Systems with External Disturbances via Variable Weighted Iterative Learning", *IEEE Transact. Circuits Syst. II: Express briefs*. https://doi.org/10.1109/TCSII.2023.3234609
Zhang, B., Han, Q., Zhang, X. and Yu, X. (2014), "Sliding mode control with mixed current and delayed states for offshore steel jacket platforms", *IEEE Transact*. *Control Syst*. *Technol*., **22**, 1769-1783. https://doi.org/10.1109/TCST.2013.2293401
Zhang, B., Han, Q. and Zhang, X. (2017), "Recent advances in vibration control of offshore platforms", *Nonlinear Dyn*., **89**, 755-771. https://doi.org/10.1007/s11071-017-3503-4
Zhang, K., Ali, A., Antonarakis, A., Moghaddam, M., Saatchi, S., Tabatabaeenejad, A. and Moorcroft, P. (2019a), "The sensitivity of North American terrestrial carbon fluxes to spatial and temporal variation in soil moisture: An analysis using radar-derived estimates of root-zone soil moisture", *J. Geophys*. *Res*.: *Biogeosci*., **124**(11), 3208-3231. https://doi.org/10.1029/2018JG004589
Zhang, K., Wang, S., Bao, H. and Zhao, X. (2019b), "Characteristics and influencing factors of rainfall-induced landslide and debris flow hazards in Shaanxi Province, China", *Natural Hazards Earth Syst*. *Sci*., **19**(1), 93-105. https://doi.org/10.5194/nhess-19-93-2019
Zhang, X., Sun, X., Lv, T., Weng, L., Chi, M., Shi, J. and Zhang, S. (2020), "Preparation of PI porous fiber membrane for recovering oil-paper insulation structure", *J. Mater. Sci.: Mater. Electron.*, **31**(16), 13344-13351. https://doi.org/10.1007/s10854-020-03888-5
Zhang, C., Kordestani, H. and Shadabfar, M. (2022a), "A combined review of vibration control strategies for high-speed trains and railway infrastructures: Challenges and solutions", *J. Low Freq. Noise Vib. Active Control*, 1420035114. https://doi.org/10.1177/14613484221128682
Zhang, Q., Wang, Z., Duan, J. and Qin, J. (2022b), "Robot motion planning with orientational constraints based on offline sampling datasets", *J. Computat. Methods Sci. Eng.*, **22**(5), 1545-1557. https://doi.org/10.3233/JCM-226140
Zhao, R., Dai, H. and Yao, H. (2022), "Liquid-metal magnetic soft robot with reprogrammable magnetization and stiffness", *IEEE Robot. Automat. Lett.*, **7**(2), 4535-4541. https://doi.org/10.1109/LRA.2022.3151164

HJ